CZECH TECHNICAL UNIVERSITY IN PRAGUE

Faculty of Nuclear Sciences and Physical Engineering

Department of Physics

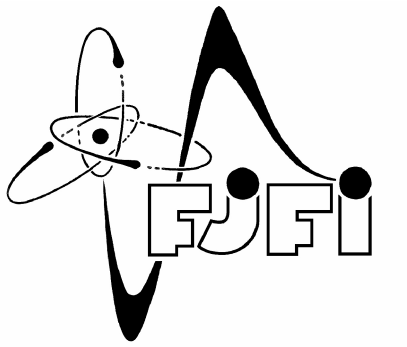

Detector control system of the ALICE TPC

Master Thesis

Martin Kroupa

Prague, 2007

Acknowledgments

I would like to express my gratitude to my supervisor Doc. RNDr. Vojtěch Petráček CSc., Dr. Luciano Musa and Dr. Chilo Garabatos for their guidance. I also want to say thank you to Prof. Peter Braun-Munzinger for his warm welcome to GSI and that he gave me this opportunity. I am also were grateful to Dr. Anton Adronic and Dr. Dariusz Miskowiecz for their guide especially in theoretical level, which helped me to understand the heavy-ion problematics better.
And at last I also want to say thank you to my parents for their support during whole studies and to Veronika for her patience and support during hard times.

Declaration of originality

I declare that I have written this diploma thesis independently using the listed references. I agree with using this diploma thesis.

Prohlašuji, že jsem svou diplomovou práci vypracoval samostatně a použil jsem pouze podklady (literaturu, projekty, SW atd.) uvedené v přiloženém seznamu.
Nemám závažný důvod proti užití tohoto školního díla ve smyslu § 60 Zákona č.121/2000 Sb., o právu autorském, o právech souvisejících s právem autorským a o změně některých zákonů (autorský zákon).

V Praze dne ....

podpis

Název práce: **Řídící systém detektrou TPC experimentu ALICE**

Autor: Martin Kroupa

Obor: Jaderné inženýrství

Druh práce: Diplomová práce

Vedoucí práce: Doc. RNDr. Vojtěch Petráček CSc. Katedra fyziky, Fakulta jaderná a fyzikálně inženýrská, České vysoké učení technické v Praze

Konzultant: Dr. Luciano Musa. ALICE TPC, CERN, Geneva

Abstrakt: Díky své schopnosti přesně rekonstruovat dráhy a energii částic je časová projekční komora (TPC) jedním z nejdůležitějších detektorů experimentu ALICE. Hlavním cílem této diplomové práce je přispění k vývoji, konstrukci a testování ovládacího systému (Detector Control System - DCS) ALICE TPC. Hlavní část práce je zaměřena na DCS pro vysoko- a nízkonapět'ové napájecí systémy, studium šumových charakteristik zdrojů napětí a jejich stabilitu. Získané výsledky prezentují důležitý přínos pro další vylepšení výkonu detektoru.

Klíčová slova: ALICE, TPC, DCS, šum.

Title: **Detector control system of the ALICE TPC**

Author: Martin Kroupa

Specialization: Nuclear Engineering

Sort of Project: Master Thesis

Supervisor: Doc. RNDr. Vojtěch Petráček CSc. Katedra fyziky, Fakulta jaderná a fyzikálně inženýrská, České vysoké učení technické v Praze

Consultant: Dr. Luciano Musa. ALICE TPC, CERN, Geneva

Abstract: The Time projection chamber (TPC) is one of the most important detectors of the ALICE experiment due to it's tracking and particle identification capabilities. The main topic of presented diploma thesis is a contribution to development, construction and commissioning of the detector control system (DCS) of the ALICE TPC. The main part of this work was concentrated on DCS for high and low voltage power supply systems, on studies of noise characteristics of power supplies and their stability. Obtained results present an important input for further improvement of the detector performance.

Keywords: ALICE, TPC, DCS, noise.

Contents

1 Introduction

The aim of high energy heavy ion physics is a study of matter at extreme conditions with very high energy densities and temperatures. Predictions say that there is a phase transition from a hadronic state to deconfined state of quarks and gluons - usually called Quark-Gluon Plasma (QGP). Exploring QGP and its properties, one can find answers to very basic questions about the early Universe. Standard Model bargain for QGP Universe shortly after Big Bang, hence higher the energies of collisions are, the farer we see to the past. Over the last decades a detailed, though still incomplete, theory

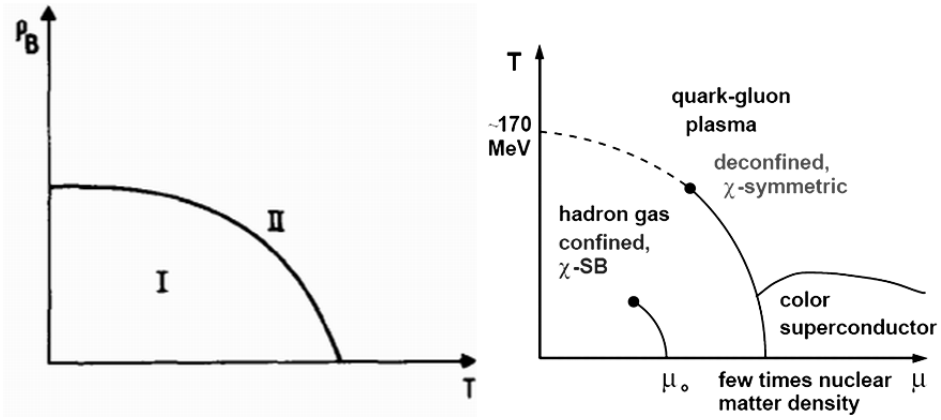

(a) The original picture of phase diagram from [1]

(b) The phase diagram today

Figure 1: Evolution of QGP phase diagram

of elementary particles and their fundamental interactions, called the Standard Model, was developed. High energy physics had the leading role in this development. Applying and extending the Standard Model to complex and dynamically evolving systems of finite size is the aim of ultra-relativistic heavy-ion physics. Understanding of collective phenomena and macroscopic properties, involving many degrees of freedom, emerge from the microscopic laws of elementary-particle physics is main contribution of heavy-ion physics. Particularly the sector of strong interactions by studying nuclear matter under conditions of extreme density and temperature is examined. The evolution of the Universe, according to Big-Bang theory, was from an initial state of extreme energy density to its present state through rapid expansion and

cooling, thereby traversing the series of phase transitions predicted by the Standard Model. Global features of our Universe, like baryon asymmetry or the large scale structure (galaxy distribution), are believed to be linked to characteristic properties of these phase transitions. Within the framework of the Standard Model, the appearance of phase transitions involving elementary quantum fields is intrinsically connected to the breaking of fundamental symmetries of nature and thus to the origin of mass. In general, intrinsic symmetries of the theory, which are valid at high-energy densities, are broken below certain critical energy densities. Particle content and particle masses originate as a direct consequence of the symmetry-breaking mechanism. Lattice calculations of Quantum Chromo Dynamics (QCD), the theory of strong interactions, predict that at a critical temperature of ~ 170 MeV, corresponding to an energy density of $\epsilon_c \sim 1$ GeV fm^{-3}, nuclear matter undergoes a phase transition to a deconfined state of quarks and gluons. In addition, chiral symmetry is approximately restored and quark masses are reduced from their large effective values in hadronic matter to their small bare ones. In ultra-relativistic heavy-ion collisions, one expects to attain energy densities which reach and exceed the critical energy density ϵ_c, thus making the QCD phase transition the only one predicted by the Standard Model that is reachable in laboratory experiments. The main objective of heavy-ion physics is to explore the phase diagram of strongly interacting mat-

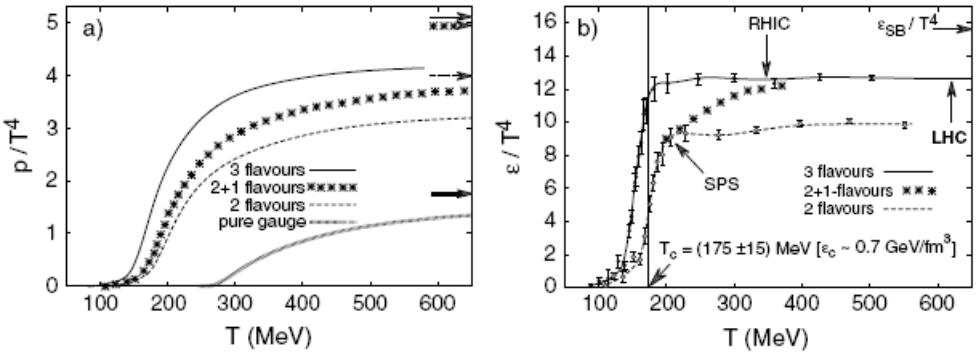

Figure 2: The pressure and energy density for different number of degenerate quarks' flavors [7]

ter, to study the QCD phase transition and the physics of the Quark-Gluon

Plasma (QGP) state. However, the system created in heavy-ion collisions undergoes a fast dynamical evolution from the extreme initial conditions to the final hadronic state. The idea of phase transition to a deconfined state is quite old. Publication with first picture of phase diagram is from 1975 [1] and you can see the original in Fig. 1. Although we know much more today, there is still no theory which can describe whole diagram. There is also uncertainty in order of phase transition. These are reasons why there are usually no numbers on axis in such a plot.
These borders were already crossed in SPS and RHIC accelerator. Bigger insight into characteristics and behavior of QGP should bring a new experiment ALICE (A Large Ion Collider Experiment).
During the last 30 years, the huge effort was made to find the ways of detecting QGP.
Direct photons, dilepton production, jets, heavy-quark and quarkonium production are only few examples of them. For more information see [3, 7].

The objective of this work was to participate in setting up and commissioning of the ALICE (A Large Ion Collider Experiment) TPC (Time Projection Chamber). The work describes wide spectrum of activities which were covered last year during precommissioning and commissioning of the TPC. Mainly describes development of part of DCS (Detector Control System), testing PSs (Power Supply) and analysis of the noise source and pattern in OROC (Outer Read-Out Chamber) chambers.

2 ALICE

During the plans for new LHC (Large Hadron Collider) accelerator, a decision was made, that one of experiments will be focused on heavy-ion program. Experience from previous projects showed that nucleus-nucleus interaction can't be extrapolated from simpler collisions. Each nucleon may scatter several times and the liberated partons from different collisions rescatter with each other even before hadronization. Hence the heavy-ion programm is quite interesting. Totally, there will be six major experiments at LHC - ALICE, ATLAS, CMS, LHCb, LHCf, TOTEM.
ATLAS and CMS have main goal in identification of Higgs boson, which gives the mass to electroweak gauge bosons using p-p collisions. They will also search for supersymmetric particles which are manifestations of a broken intrinsic symmetry between fermions and bosons in extensions of the Standard Model. LHCb, focusing on precision measurements with heavy b quarks, will study CP-symmetry violating processes. The ALICE program will be focused on studying QGP behavior and to study the role of chiral symmetry in the generation of mass in composite particles (hadrons). The nucleon-nucleon center-of-mass energy for collisions of the heavy ions at the LHC ($\sqrt{s} = 5.5$ TeV) will exceed that available at RHIC by a factor of about 30.
In order to be able to measure all interesting processes is the ALICE combined from three major components:

- Central barrel, contained in L3 magnet composed from detectors used to study hadronic signals and dielectrons (pseudorapidity region -0.9 $< \eta <$ 0.9)
- Forward muon spectrometer studying muon pairs from decay of quarkonia (pseudorapidity region 2.5 $< \eta <$ 4.0)
- Forward detectors for photon and charged particles multiplicity determination, will be also used as a fast trigger on the centrality of collision (pseudorapidity region $\eta >$ 4)

	SPS	RHIC	LHC
E_{cm} [GeV]	17	200	5500
dN_{ch}/dy	500	700	2000 - 8000
ϵ [Gev/fm^3]$_{t_0=1fm/c}$	$\approx$ 2.5	$\approx$ 3.5	$\approx$ 15 - 40
V_{freeze}[fm^3]	$\approx 10^3$	$\approx 7{\cdot}10^3$	$\approx 2{\cdot}10^4$ - $5{\cdot}10^4$
τ_{QGP} [fm/c]	< 1	1.5 - 4	4 - 10

Table 1: Accelerator's parameters

The ALICE is built in consideration of possible upgrading of detector, because how we saw in the past new signals of QGP or new ways of their detecting can appear.

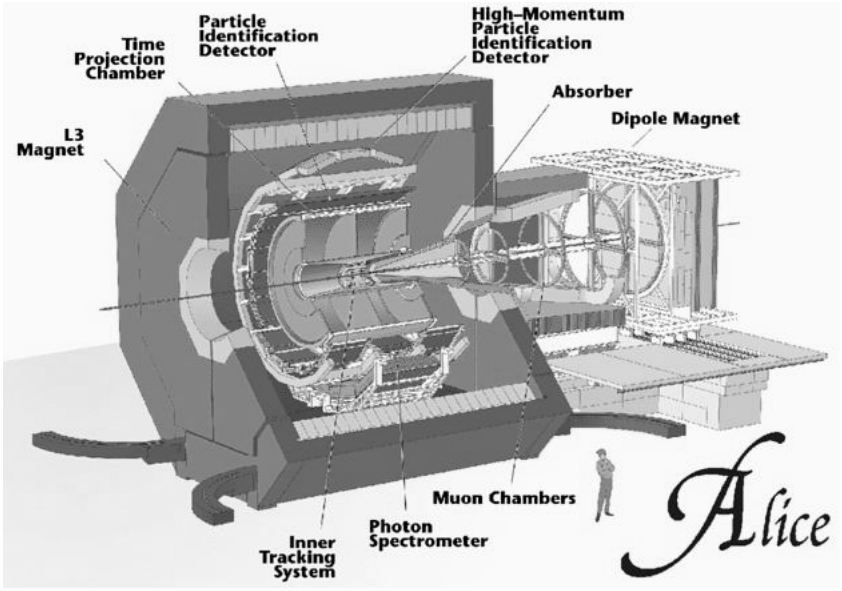

Figure 3: Layout of the ALICE experiment[3]

2.1 Detectors of the ALICE

ITS

The Inner Tracking System (ITS) consists of six cylindrical layers of silicon detectors, located at radii, r = 4, 7, 15, 24, 39 and 44 cm. It covers the rapidity range of $|\eta| < 0.9$ for all vertices located within the length of the

interaction diamond ($\pm 1\sigma$), i.e. 10.6 cm along the beam direction. The number, position and segmentation of the layers are optimized for efficient track finding and high impact-parameter resolution. In particular, the outer radius is determined by the necessity to match tracks with those from the Time-Projection Chamber (TPC), and the inner radius is the minimum allowed by the radius of the beam pipe (3 cm). The first layer has a more extended coverage ($|\eta| < 1.98$) to provide, together with the Forward Multiplicity Detectors (FMD), a continuous coverage in rapidity for the measurement of charged-particles multiplicity. Because of the high particle density, up to 80 particles cm^{-2}, and to achieve the required impact parameter resolution, pixel detectors have been chosen for the innermost two layers, and silicon drift detectors for the following two layers. The outer two layers, where the track densities are below 1 particle cm^2, will be equipped with double-sided silicon micro-strip detectors. With the exception of the two innermost pixel planes, all layers will have analogue readout for particle identification via dE/dx measurement in the non-relativistic ($1/\beta^2$) region. This will give the ITS a stand-alone capability as a low-p_t particle spectrometer.[3]

TPC

The Time-Projection Chamber (TPC) is the main tracking detector of the ALICE central barrel and, together with the other central barrel detectors has to provide charged-particle momentum measurements with good two-track separation, particle identification, and vertex determination. The phase space covered by the TPC ranges in pseudo-rapidity $|\eta| < 0.9$ (up to $|\eta| \sim 1.5$ for tracks with reduced track length and momentum resolution); in p_T up to 100 GeV c^{-1} is reached with good momentum resolution. In addition, data from the central barrel detectors will be used to generate a fast online High-Level Trigger (HLT) for the selection of low cross-section signals. All these requirements need to be fulfilled at the PbŰPb design luminosity, corresponding to an interaction rate of 8 kHz, of which about 10% are to be considered as central collisions. For these we assume the extreme multiplicity of $dN_{ch}/d\eta = 8000$, resulting in 20 000 charged primary and secondary tracks in the acceptance, an unprecedented track density for the TPC. These

extreme multiplicities set new demands on the design which were addressed by extensive R&D activities; test beam results show a good performance even at the highest anticipated multiplicities. Careful optimization of the TPC design finally resulted in maximum occupancies (defined as the ratio of the number of readout pads and time bins above threshold to all pads and time bins) of about 40% at the innermost radius and 15% at the outermost radius. Substantial improvements in the tracking software were necessary to achieve adequate tracking efficiency under such harsh conditions; tracking efficiencies ∼90% were obtained for primary tracks at the time of the TPC TDR and they have improved further recently. For proton-proton runs, the memory time of the TPC is the limiting factor for the luminosity due to the ∼90 μs drift time. At a pp luminosity of about 5×10^{30} cm^{-2} s^{-1}, with a corresponding interaction rate of about 350 kHz, past and future tracks from an average of 60 pp interactions are detected together with the triggered event; the detected multiplicity corresponds to about 30 minimum-bias pp events. The total occupancy, however, is lower by more than an order of magnitude than in Pb-Pb collisions, since the average pp multiplicity is about a factor 10^3 lower than the Pb-Pb multiplicity for central collisions. Tracks from pile-up events can be eliminated because of their wrong vertex pointing.[3]

Transition-Radiation Detector

The main goal of the ALICE Transition-Radiation Detector (TRD) is to provide electron identification in the central barrel for momenta greater than 1 GeV c^{-1}, where the pion rejection capability through energy loss measurement in the TPC is no longer sufficient. As a consequence, the addition of the TRD significantly expands the ALICE physics objectives. The TRD will provide, along with data from the TPC and ITS, sufficient electron identification to measure the production of light and heavy vector-meson resonances and the dilepton continuum in PbŰPb and pp collisions. In addition, the electron identification provided by the TPC and TRD for p_t >1 GeV c^{-1} can be used, in conjunction with the impact-parameter determination of electron tracks in the ITS, to measure open charm and open beauty produced in the collisions. A similar technique can be used to separate directly produced

J/ψ mesons from those produced in B-decays. These secondary J/ψŠs could potentially mask the expected J/ψ yield modification due to quarkŰgluon plasma formation; their isolation is, therefore, of crucial importance for such measurements. Furthermore, since the TRD is a fast tracker, it can be used as an efficient trigger for high transverse momentum electrons. Such a trigger would considerably enhance the recorded Υ yields in the high-mass part of the dilepton continuum as well as high-p_t J/ψ.[3]

Time-Of-Flight

The Time-Of-Flight (TOF) detector of the ALICE is a large area array that covers the central pseudo-rapidity region ($|\eta| < 0.9$) for Particle IdDntification (PID) in the intermediate momentum range (from 0.2 to 2.5 GeV c^{-1}). Since the majority of the produced charged particles is emitted in this range, the performance of such a detector is of crucial importance for the experiment. The measurement and identification of charged particles in the intermediate momentum range will provide observables which can be used to probe the nature and dynamical evolution of the system produced in ultra-relativistic heavy-ion collisions at LHC energies. The TOF, coupled with the ITS and the TPC for track and vertex reconstruction and for dE/dx measurements in the low-momentum range (up to about 0.5 GeV c^{-1}), will provide event-by-event identification of large samples of pions, kaons, and protons. The TOF-identified particles will be used to study relevant hadronic observables on a single-event basis. In addition, at the inclusive level, identified kaons will allow invariant mass studies, in particular the detection of open charm states and the ϕ meson. A large-coverage, powerful TOF detector, operating efficiently in extreme multiplicity conditions, should have an excellent intrinsic response and an overall occupancy not exceeding the 10-15% level at the highest expected charged-particle density ($dN_{ch}/d\eta = 8000$). This implies a design with more than 10^5 independent TOF channels. Since a large area has to be covered, a gaseous detector is the only choice. In the framework of the LAA project at CERN an intensive R&D program has shown that the best solution for the TOF detector is the Multi-gap Resistive-Plate Chamber (MRPC). The key aspect of these chambers is that the electric field is high

and uniform over the whole sensitive gaseous volume of the detector. Any ionization produced by a traversing charged particle will immediately start a gas avalanche process which will eventually generate the observed signals on the pick-up electrodes. There is no drift time associated with the movement of the electrons to a region of high electric field. Thus the time jitter of these devices is caused by the fluctuations in the growth of the avalanche.[3]

High-Momentum Particle Identification Detector

The High-Momentum Particle Identification Detector (HMPID), is dedicated to inclusive measurements of identified hadrons for p_t >1 GeV c^{-1}. The HMPID was designed as a single-arm array with an acceptance of 5% of the central barrel phase space. The geometry of the detector was optimized with respect to particle yields at high-p_t in both pp and heavy-ion collisions at LHC energies, and with respect to the large opening angle (corresponding to small effective size particle emitting sources) required for two-particle correlation measurements. HMPID will enhance the PID capability of the ALICE experiment by enabling identification of particles beyond the momentum interval attainable through energy loss (in the ITS and the TPC) and time-of-flight measurements (in TOF). The detector was optimized to extend the useful range for π/K and K/p discrimination, on a track-by-track basis, up to 3 and 5 GeV c^{-1} respectively.[3]

PHOton Spectrometer

The PHOton Spectrometer (PHOS) is a high-resolution electromagnetic spectrometer which will detect electromagnetic particles in a limited acceptance domain at central rapidity and provide photon identification as well as neutral mesons identification through the two-photon decay channel.[3]

ElectroMagnetic CAlorimeter (EMCA)

Each EMCA module is segmented into 3584 detection channels arranged in 56 rows of 64 channels. The detection channel consists of a 22×22×180 mm^3 lead-tungstate crystal, $PbWO_4$(PWO), coupled to a 5×5 mm^2 Avalanche Photo-Diode (APD) which signal is processed by a low-noise preamplifier.

The total number of crystals in PHOS is 17 920 representing a total volume of $\sim 1.5\text{m}^3$. The main mechanical assembly units in a module is the crystal strip unit consisting of eight crystal detector units forming 1/8 of a row. The APD and the preamplifier are integrated in a common body glued onto the end face of the crystal with optically transparent glue of a high refractive index. To significantly (by about a factor of 3) increase the light yield of the PWO crystals (temperature coefficient $\sim$-2% per °C), the EMCA modules will be operated at a temperature of -25 °C. The temperature will be stabilized with a precision of $\sim$0.3 °C. To this purpose, the EMCA module is subdivided by thermo-insulation into a cold and warm volume. The crystal strips will be located in the cold volume, whereas the readout electronics will be located outside this volume. All six sides of the cold volume will be equipped with cooling panels, and heat is removed by a liquid coolant (hydrofluoroether) pumped through the channels of these panels. Temperature monitoring will be provided by means of a temperature measurement system, based on resistive temperature sensors of thickness 30-50 μm, which will be inserted in the gap between crystals. A monitoring system using Light Emitting Diodes (LED) and stable current generators will monitor every EMCA detection channel. The system consists of Master Modules (MM) and Control Modules (CM). The MM (one per PHOS module) are located in the pit in the same VME crate as the PHOS trigger electronics. For each EMCA module there are 16 CM boards, located in the ŚcoldŠ volume of the EMCA modules, directly on top of the crystals. Each board, placed on a 15mm thick NOMEX plate, is equipped with a 16×14 LED matrix and the control and decoding circuits.[3]

Forward Muon Spectrometer

Hard, penetrating probes, such as heavy-quarkonia states, are an essential tool for probing the early and hot stage of heavy-ion collisions. At LHC energies, energy densities high enough to melt the Υ(1s) will be reached. Moreover, production mechanisms other than hard scattering might play a role. Since these additional mechanisms strongly depend on charm multiplicity, measurements of open charm and open beauty are of crucial importance

(the latter also represents a potential normalization for bottomium). The complete spectrum of heavy quark vector mesons (i.e. J/ψ, ψ', Υ, Υ' and Υ''), as well as the ϕ meson, will be measured in the $\mu^+\mu^-$ decay channel by the ALICE muon spectrometer. The simultaneous measurement of all the quarkonia species with the same apparatus will allow a direct comparison of their production rate as a function of different parameters such as transverse momentum and collision centrality. In addition to vector mesons, also the unlike-sign dimuon continuum up to masses around 10 GeV c^{-2} will be studied. Since at LHC energies the continuum is expected to be dominated by muons from the semi-leptonic decay of open charm and open beauty, it will also be possible to study the production of open (heavy) flavours with the muon spectrometer. Heavy-flavour production in the region -2.5 $< \eta <$ -1 will be accessible through measurement of e-μ coincidences, where the muon is detected by the muon spectrometer and the electron by the TRD.[3]

Zero-Degree Calorimeter

The observable most directly related to the geometry of the collision is the number of participant nucleons, which can be estimated by measuring the energy carried in the forward direction (at zero degree relative to the beam direction) by non-interacting (spectator) nucleons. The zero degree forward energy decreases with increasing centrality. Spectator nucleons will be detected in the ALICE by means of Zero-Degree Calorimeters (ZDC).

Photon Multiplicity Detector

The Photon Multiplicity Detector (PMD) is a preshower detector that measures the multiplicity and spatial (η-φ) distribution of photons on an event-by-event basis in the forward region of the ALICE. The PMD addresses physics issues related to event-by-event fluctuations, flow and formation of Disoriented Chiral Condensates (DCC) and provides estimates of transverse electromagnetic energy and the reaction plane on an event-by-event basis.[3]

Forward Multiplicity Detector

The main functionality of the silicon strip Forward Multiplicity Detector

(FMD) is to provide (offline) charged-particle multiplicity information in the pseudo-rapidity range -3.4 $< \eta <$ -1.7 and 1.7 $< \eta <$ 5.1. The FMD will allow for the study of multiplicity fluctuations on an event-by-event basis and for flow analysis (relying on the azimuthal segmentation) in the considered pseudo-rapidity range. Together with the pixel system of the ITS, the FMD will provide early charged particle multiplicity distributions for all collision types in the range -3.4 $< \eta <$ 5.1. Overlap between the various rings and with the ITS inner pixel layer provides redundancy and important checks of analysis procedures.[3]

V0 detector

The V0 detector has multiple roles. It provides:

- a minimum bias trigger for the central barrel detectors
- two centrality triggers in Pb-Pb collisions
- a centrality indicator
- a control of the luminosity
- a validation signal for the muon trigger to filter background in pp mode

Special care must be taken to minimize the background due to the location of the V0 detector. Indeed, the presence of important material volumes (beam pipe, front absorber, FMD, T0, ITS services) in front of the V0 arrays will generate an important number of secondaries (mainly electrons) which will affect physical information about the number of charged particles. The efficiency of minimum bias triggering and the multiplicity measurement will be strongly modified by this secondary particle production. Beam–gas interactions will be another source of background. It will provide triggers which have to be identified and eliminated. This background is particularly important in pp runs. Measuring the time-of-flight difference between two detectors located on each side of the interaction point will enable to identify these background events. The V0 detector must therefore provide signal charge and time-of-flight measurement capabilities.[3]

T0 detector

The T0 detector has to perform the following functions:

- To generate a T0 signal for the TOF detector. This timing signal corresponds to the real time of the collision (plus a fixed time delay) and is independent on the position of the vertex The required precision of the T0 signal is about 50 ps (r.m.s.).
- To measure the vertex position (with a precision ± 1.5 cm) for each interaction and to provide a L0 trigger when the position is within the preset values. This will discriminate against beam-gas interactions.
- To provide an early 'wake-up' signal to TRD, prior to L0.
- To measure the particle multiplicity and generate one of the three possible trigger signals: $T0_{min-bias}$, $T0_{semi-central}$, or $T0_{central}$.

Since the T0 detector generates the earliest L0 trigger signals, they must be generated online without the possibility of any offline corrections. The dead time of the detector should be less than the bunch-crossing period in pp collisions (25 ns).[3]

Cosmic-ray trigger detector

The cosmic-ray trigger for the ALICE will be part of ACORDE (A COsmic Ray DEtector for the ALICE) which together with some other ALICE tracking detectors, will provide precise information on cosmic rays with primary energies around 10^{15}-10^{17} eV. The Cosmic-Ray Trigger (CRT) system will provide a fast L0 trigger signal to the central trigger processor, when atmospheric muons impinge upon the ALICE detector. The signal will be useful for calibration, alignment and performance of several ALICE tracking detectors, mainly the TPC and the ITS. The cosmic-ray trigger signal will be capable to deliver a signal before and during the operation of the LHC beam. The typical rate for single atmospheric muons crossing the ALICE cavern will be less than 3-4 Hz m^{-2}. The rate for multi-muon events will be lower (less than 0.04 Hz m^{-2}) but sufficient for the study of these events provided that one can trigger and store tracking information from cosmic

muons in parallel to the ALICE normal data taking with colliding beams. The energy threshold of cosmic muons arriving to the ALICE hall is approximately 17 GeV, while the upper energy limit for reconstructed muons will be less than 2 TeV, depending of the magnetic field intensity (up to 0.5 T).[3]

3 TPC

The TPC (Time Projection Chamber) is gas drift detector. Cylindrical in shape the TPC has an inner radius of about 85 cm, an outer radius of about 250 cm. Overall length along the beam direction is 500 cm. With volume 88 m^3 is the ALICE TPC (Fig. 4) the biggest TPC ever built. The cylindrical field cage, is filled of gas mixture of 90% Ne and 10% CO_2 which causes that high voltage is needed. On central electrode is 100 kV and the field

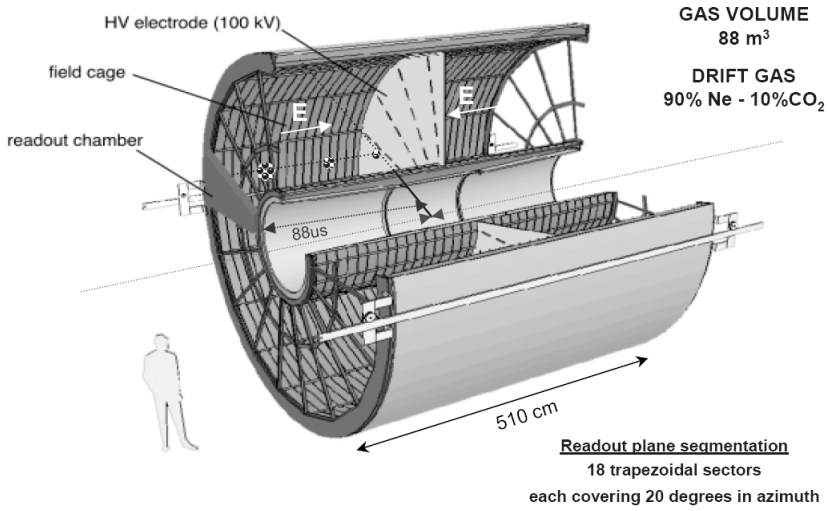

Figure 4: Layout of the ALICE TPC [4]

inside cylinder is 400 V/cm. This gas was chosen because of his long term stability (opposite to CF_4 and CH_4 with ageing properties). This mixture is also optimized for drift velocity, low diffusion, low radiation length and hence low multiple scattering and small space-charge effect. Recently the idea of including N_2 was considered. Mixture Ne-Co_2-N_2 90-10-5 was tested as the best one. This would make the TPC less sensitive to nitrogen accumulation and makes stable gain two-times higher. On the other hand higher voltage has to be connected to wire chambers to get same gain (the chambers are capable of this) (Fig. 7). The gas composition and purity play one of main roles. Even very small amount of oxygen or water can rapidly lower resolution and response of the detector (electron attachment). Hence precise

and rather complicated gas system was developed. The gas composition is monitored online and the gas is filtered and cleaned all the time. In order to be able to compute the gas composition online, the small model of the TPC was made (called GOOFIE) and plugged to the gas system circuit. On this model one can measure the drift velocity as it is in the real TPC. As was mentioned above the oxygen can make unacceptable problems, that's why maximum allowed amount of oxygen within demanded physical conditions is 5 ppm, but in normal conditions should be around 1 ppm. As a protection against leaking the outer space around the TPC is filled with CO_2. Once the charged particle crosses volume of the detector it ionizes the gas inside. Created electrons drift to anode plane which is on the end of the TPC, ions drift to the central cathode. Read-out is done via multi-wire proportional chambers (MWPC) with cathode padplane on end plates. Time needed to transport the primary electrons over a distance of up to 2.5m on either side of the central electrode to the end-plates is around 90 μs. The multi-wire proportional chambers with cathode pad readout are mounted into 18 trapezoidal sectors of each end-plate. High electric field density in the end of

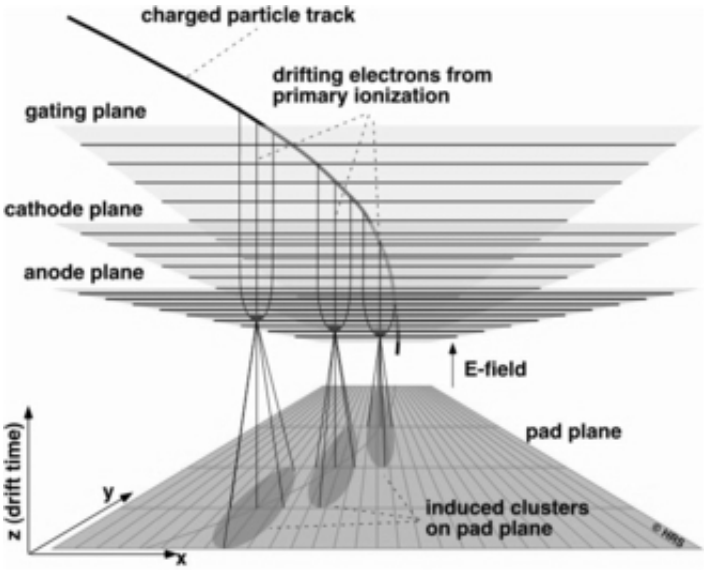

Figure 5: Layout of read-out on pad plane of the ALICE TPC [3]

the drift region causes that electron avalanches occur. These avalanches are

collected on anodes and projection charge is read from pad plane (Fig. 5). From the position of the pad planes and the drift time one can reconstruct particle track in 3D. To improve the resolution of the detector gating grid is part of the chamber. It is used for triggering (only opens when trigger arrives) and for preventing of accumulation charged ions in drift volume. This is very important in the ALICE where will be high multiplicity. Example of the electric field around the gating grid is in Fig. 6. One has to mention that the geometry of the wire chamber is very complicated thing. Changing wires' diameter and distance among them cause changing in the position resolution and two tracks resolution. The geometry of pads is also very important. During development of the TPC many configurations were tested, more, including all numbers, one can find in [4]. The ALICE TPC

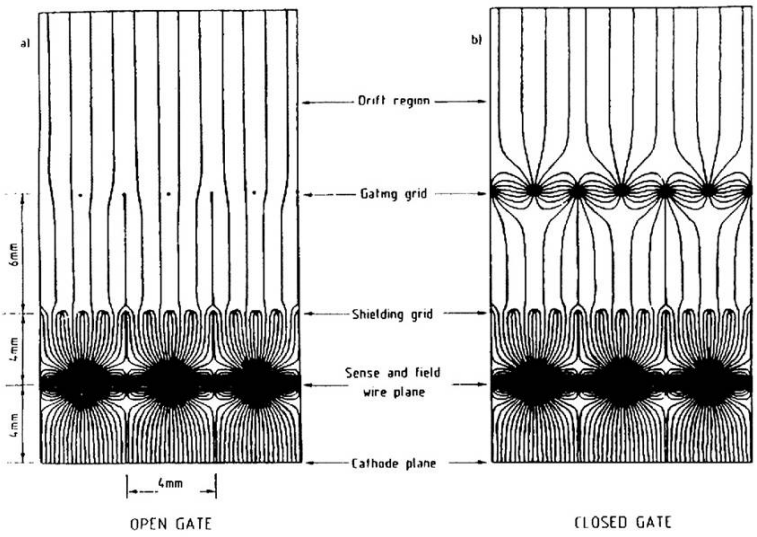

Figure 6: Example of electric field around gating grid

is not only a main tracking detector capable of precision paths identification of charged particles in 3D, but also measuring of their energy loses and thus their identification. [3, 4]

Whole system depends strongly on gas purity, temperature and pressure. As was mentioned on each endplate there are 18 chambers with total 570312

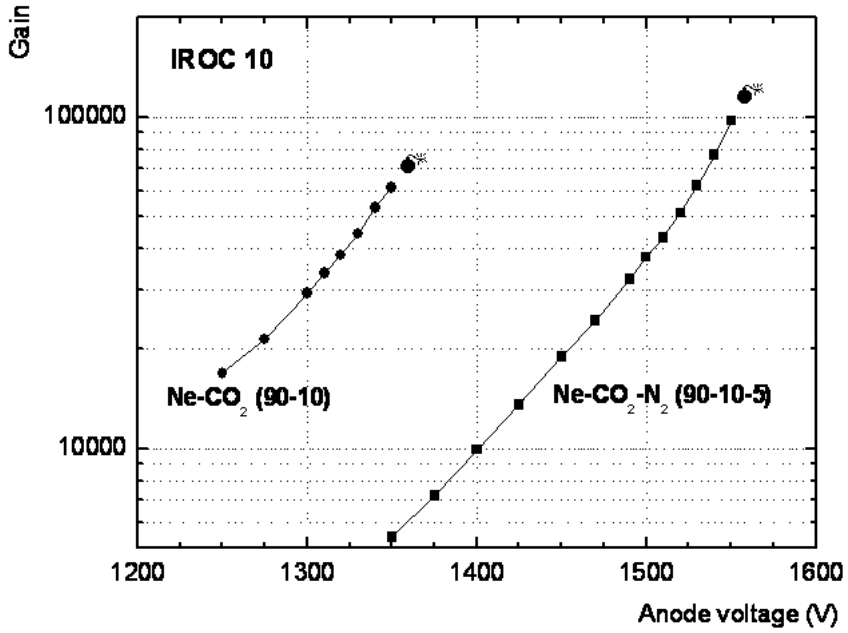

Figure 7: Gain comparasion for gas without and with nitrogen

charge sensitive read-out pads. In order to cover different demands in radius direction (different track density), every chamber is divided into two independent pars: Inner Read-Out Chamber (IROC) and Outer Read-Out Chamber (OROC). This two differ in geometry of wires and their parameters as well as in pad size. To keep the occupancy as low as possible and to ensure the necessary dE/dx and position resolution, there are readout pads of three different sizes: 4x7.5 mm^2 in the inner chambers, 6x10 and 6x15 mm^2 in the outer chambers. In normal state the read-out chambers are closed from drift volume by gating grid. Gating grid is opened only when trigger L1 arrives and it is opened for around 100μs. [3, 4, 7].
The summary of the TPC parameters is in Fig. 8

3.1 Front End Electronics (FEE)

The front-end electronics has to read out the charge detected by readout chambers at the TPC end-caps. A current signal has a fast rise time (less

Pseudo-rapidity coverage	$-0.9 < \eta < 0.9$ for full radial track length
	$-1.5 < \eta < 1.5$ for 1/3 radial track length
Azimuthal coverage	2π
Radial position (active volume)	$845 < r < 2466$ mm
Radial size of vessel	$780 < r < 2780$ mm
Length (active volume)	5000 mm
Segmentation in φ	18 sectors
Segmentation in r	Two chambers per sector
Segmentation in z	Central membrane, readout on two end-plates
Total number of readout chambers	$2 \times 2 \times 18 = 72$
Inner readout chamber geometry	Trapezoidal, $848 < r < 1320$ mm active area
Pad size	4×7.5 mm ($\varphi \times r$)
Pad rows	63
Total pads	5504
Outer readout chamber geometry	Trapezoidal, $1346 < r < 2466$ mm active area
Pad size	6×10 and 6×15 mm ($\varphi \times r$)
Pad rows	64+32 = 96 (small and large pads)
Total pads	4864+5120 = 9984 (small and large pads)
Detector gas	Ne/CO_2 90/10
Gas volume	88 m^3
Drift length	2×2500 mm
Drift field	400 V cm^{-1}
Drift velocity	2.84 cm μs^{-1}
Maximum drift time	88 μs
Total HV	100 kV
Diffusion	$D_L = D_T = 220\ \mu$m $cm^{-1/2}$
Material budget	$X/X_0 = 3.5$ to 5% for $0 < \lvert\eta\rvert < 0.9$
Front-End Cards (FEC)	121 per sector $\times$ 36 = 4356
Readout Control Unit (RCU) scheme	6 per sector, 18 to 25 FEC per RCU
Total RCUs	216
Total pads — readout channels	557 568
Pad occupancy (for $dN/dy = 8\,000$)	40–15% (inner/outer radius)
Pad occupancy (for pp)	$5–2 \times 10^{-4}$ (inner/outer radius)
Event size (for $dN/dy = 8000$)	~60 MB
Event size (for pp)	~1–2 MB depending on pile-up
Data rate limit	400 Hz Pb–Pb minimum bias events
Trigger rate limits	200 Hz Pb–Pb central events
	1000 Hz proton–proton events
ADC	10 bit
Sampling frequency	5.7–11.4 MHz
Time samples	500–1000
Conversion gain	6 ADC counts fC^{-1}
Position resolution (σ)	
In $r\varphi$	1100–800 μm (inner/outer radii)
In z	1250–1100 μm
dE/dx resolution	
Isolated tracks	5.5%
$dN/dy = 8000$	6.9%

Figure 8: Parameters of the ALICE TPC [7]

than 1 ns), and a long tail due to the motion of the positive ions. The amplitude, which is different for the different pad sizes, has a typical value of 7 μA. The signal is delivered on the detector impedance, to a very good approximation a pure capacitance of the order of a few pF. A single readout channel is comprised of three basic functional units:

- a charge sensitive amplifier/shaper (PASA)
- a 10-bit 10-MSPS low-power ADC
- a digital circuit that contains a shortening filter for the tail cancellation, baseline subtraction and zero-suppression circuits, and a multiple-event buffer

The schematic of signal processing is in Fig. 9. The main requirements for

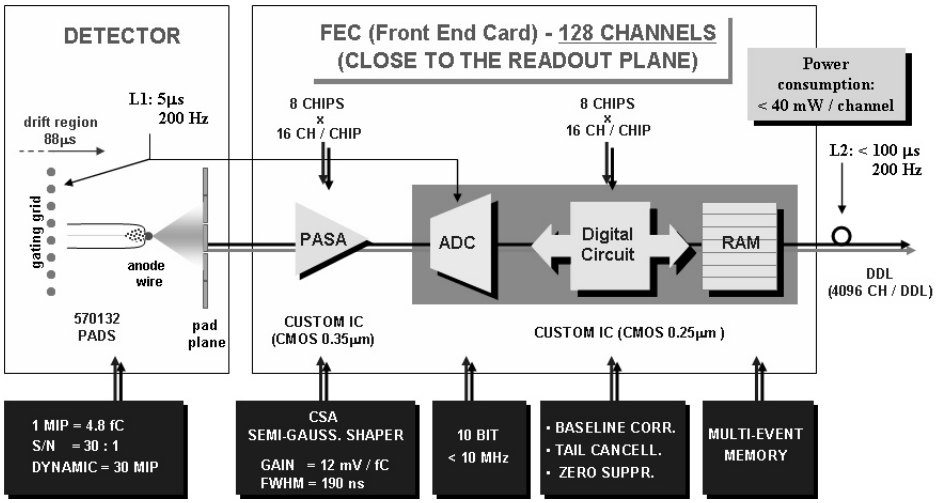

Figure 9: Schematic of signal processing [4]

the readout electronics are in Tab. 2. They are briefly discussed bellow:

- Monte Carlo studies indicate that to reach the detector resolution a signal-to-noise ratio 30:1 is needed
- The maximum pad and time bin for a hit corresponds typically to a charge of about 4.8 fC (3 x 10^4 electrons) for a minimum ionizing

particle, leading to a maximum acceptable noise (r.m.s.) of about 1000 electrons.

- In order to avoid the saturation caused by energetic particles and Landau fluctuation (up to 30 MIP), dynamic range should be at least 10 bits.

- The amplifier conversion gain has to be such that the maximum output signal matches the input dynamic range of the ADC. An ADC with 2 V dynamic range, e.g., requires a conversion gain of about 12 mV/fC.

- Shaping time has to be compromise between the achieving high signal-to-noise ratio, which is very bandwidth consuming and overlap of successive signals. Shaping time about 200 ns is this compromise.

- The shaping time of about 200 ns makes a sampling frequency of 5Ű6 MHz plausible. We therefore divide the total drift time of 88 μs into about 500 time bins, leading to a sampling frequency of 5.66 MHz. Each of the 500 time bins corresponds to a drift distance of 5 mm. (today used 10 MHz and 1000 bins)

- Owing to the high channel occupancy, in order to minimize pile-up effects, a very precise tail cancellation, at the level of 0.1% of the maximum pulse height, is required in the front-end stage. This can be done either before or after the analog-to-digital conversion.

- The large granularity or the TPC (3 x 10^8 pixels for 500 time bins) leads to event sizes of about 84 MByte after zero suppression. Hence the zero suppression before transfer to DAQ is necessary. Zero suppression at the front-end will reduce the data volume by a factor 2.5, leading to a data throughput of 8.4 GByte/s with 100 events/s transferred to the DAQ/Level-3 processing.

- A critical aspect in the TPC operation is the temperature stability. To ensure a constant drift velocity it has to be controlled at the level of about 0.1° C (drift velocity depends strongly on temperature $\sim$ T^4)

Parameter	Value
Number of channels	570132
Signal to noise ratio	30:1
Dynamic range	900:1
Noise (ENC)	1000e
Conversion gain	12mV/fC
Crosstalk	$< 0.3\%$
Shaping time	about 200 ns
Sampling rate	5-12 MHz
Tail correction after 1 μs	0.1%
Bandwidth to DAQ/Level-3	8.4 GByte/s
Maximum dead time	10%
Power consumption	$<$ 100 mW/channel

Table 2: Front-end electronics requirements [4]

over the whole volume. Because of a large number of channels the power consumption should be kept as low as possible. The aim is to keep the total power consumption below 60 kW (100 mW/channel).

- The radiation load on the TPC is low, with a total dose received over 10 years of less than 300 rad and a neutron flux of less than 10^{11} neutrons/cm^2. Thus standard radiation-soft technologies are suitable for the implementation of this electronics. Nevertheless, some special care should be taken to protect the system against potential damage caused by Single Event Effects (SEEs).

- The electronics will be located in an area with limited access. High reliability is thus a concern. [3, 4, 7]

3.2 FEC

The FEC contains the complete read-out chain. As was mentioned above each channel consists from three main parts - charge sensitive PreAmplifier/ShAper (PASA), 10-bit 10 MHz low-power ADC and circuits for tail cancellation, the baseline subtraction, zero-suppression and multiple-event

buffer. ADC and circuits are contained in one chip named ALTRO. ((ALice Tpc ReadOut). The FEC receives 128 analogue signals through 6 flexible kapton cables and the corresponding connectors. The input signals are very fast, with a rise time of less than 1ns. Therefore, to minimize the channel-to-channel crosstalk, the 8 PASA circuits have to be very close to the input connectors. [8, 4]

PASA

Each PASA contains shaping-amplifier circuits for 16 channels. Charge sensitive amplifier is followed by a semi-Gaussian pulse shaper of the 4^{th} order. For these analogue circuits th 0.35 μm CMOS technology is used. The power consumption is 11 mW/channel. The circuit has a conversion gain of 12 mV/fC and an output dynamic range of 2 V with a differential non-linearity of 0.2%. It produces a pulse (Fig. 10) with a shaping time (FWHM) of 190 ns. The single channel has a noise value below 570 e- (r.m.s.) and a channel-to-channel crossŰtalk below -60 dB. [3, 8]

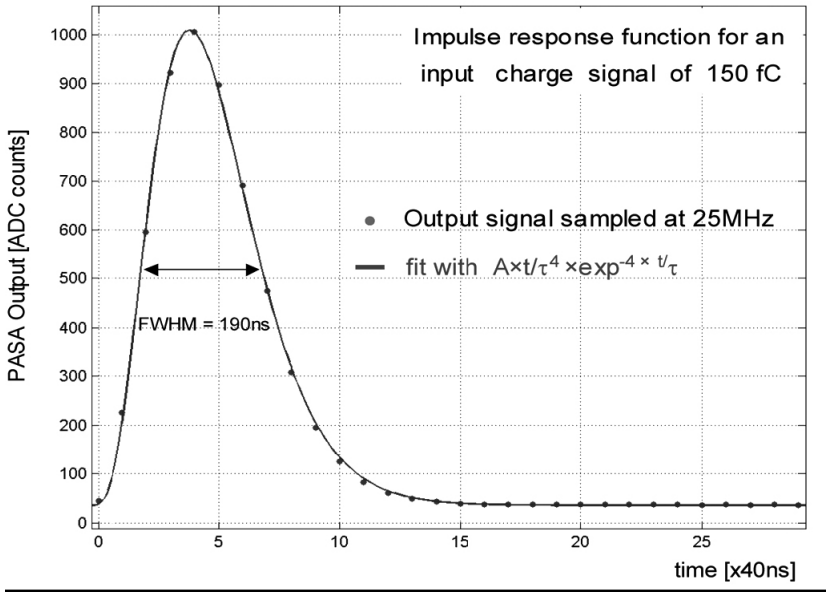

Figure 10: PASA impulse response function for a input charge of 150 fC. [8]

ALTRO

This special chip is integrating 16 channels each with 10-bit pipelined ADC

(one per channel) with sampling frequency 5-12 MHz, a pipelined Digital Processor and multi-acquisition Data Memory. Memory is used for storage events after L-1 trigger. The data are stored till L-2 trigger arrives or are overwritten by the new events. Several algorithms are used to condition and shape the signal. After digitization, the Baseline Correction Unit I is able to perform channel-to-channel gain equalization and to correct for possible non-linearity and baseline drift of the input signal. It is also able to adjust DC levels and to remove systematic spurious signals by subtracting a pattern stored in a dedicated memory. The next processing block is an 18-bit, fixed-point arithmetic, 3rd order Tail Cancellation Filter. The latter is able to suppress the signal tail, within 1 ìs after the pulse peak, with the accuracy of 1 LSB. Since the coefficients of this filter are fully programmable, the circuit is able to cancel a wide range of signal tail shapes. Moreover, these coefficients can be set independently for each channel and are re-configurable. This feature allows a constant quality of the output signal regardless of ageing effects on the detector and/or channel-to-channel fluctuations. The subsequent processing block, Baseline Correction Unit II, applies a baseline correction scheme based on a moving average filter. [8] After this the Zero-Suppression procedure is started. All data bellow programmable threshold are discarded, thus the data volume is significantly decreased. After these procedures data are stored in buffer where from four 10-bit words new 40-bit word is created and send to DAQ. Consequences of this are rather unexpected and will be discussed later in section 5.

3.3 RCU

The Read-Out Control Unit (RCU) is motherboard card 22.5×15 cm^2. The RCU interfaces the FECs to the Data Acquisition System (DAQ), the Timing and Trigger System (TTC) and the Detector Control System (DCS). The RCU broadcasts the trigger information to the FECs, collects the trigger-related data from the FECs, assembles a sub-event, compresses the data and sends the compressed packed subevent to the DAQ via optical fiber, the ALICE Detector Data Link (DDL). Moreover, the RCU has to initialize the

FECs and monitor their behavior reporting to the DCS any detected fault.[11] The RCU hosts two mezzazine cards DCS with TTCrx which produces the phase-corrected LHC clock, Level-1 trigger and Level-2 accept/reject. These are used on the RCU, and also distributed to all the FECs via the ALTRO bus. In addition, the TTCrx delivers event identification information to be added to the sub-event header before sending the data to the DDL. From technical point of view is DCS card Linux PC. One can communicate with it via ethernet.
Second card is SIU (Source Interface Unit), which is responsible to communication with DAQ. Optical fibers DDL are connected to this card and allows two way communication with RORC card implemented in DAQ PC. RCU is also storage for settings of FECs (i.e. pedestals).
The RCU is responsible for reading out the front end electronics. The RCUs are situated just outside the TPC and are connected to 18-25 front end cards. A total of six RCUs is necessary in order to read out one TPC sector (4 OROC+2 IROC). Before reading out data the RCU must be configured properly. The configuration of the FECs is the responsibility of the RCU. The RCU can be configured via the DDL links or via the DCS board connected to it. [10, 11]

3.4 DAQ

The architecture of the data acquisition is shown in Fig. 11. The detectors receive the trigger signals and the associated information from the Central Trigger Processor (CTP), through a dedicated Local Trigger Unit (LTU) interfaced to a Timing, Trigger and Control (TTC) system. The readout electronics of the detectors is interfaced to the ALICE-standard Detector Data Links (DDL). The data produced by the detectors (event fragments) are injected on the DDLs using the same standard protocol. The fact that all the detectors use the DDL is one of the major architectural features of the ALICE DAQ. At the receiving side of the DDLs there are PCI-based electronic modules, called 'DAQ Readout Receiver Card' (D-RORC). The D-RORCs are hosted by the front-end machines (commodity PCs), called

Local Data Concentrators (LDCs). Each LDC can handle one or more D-RORCs. The D-RORCs perform concurrent and autonomous DMA transfers into the LDCs' memory, with minimal software intervention. The event fragments originated by the various D-RORCs are logically assembled into sub-events in the LDCs. The CTP receives a busy signal from each detector. This signal can be generated either in the detector electronics or from all the D-RORCs of a detector. The CTP also receives a signal from the DAQ enabling or disabling the most common triggers. It is used to increase the acceptance of rare triggers by reducing the detector dead-time. This signal is generated from the buffer occupancy in all the LDCs. The role of the LDCs

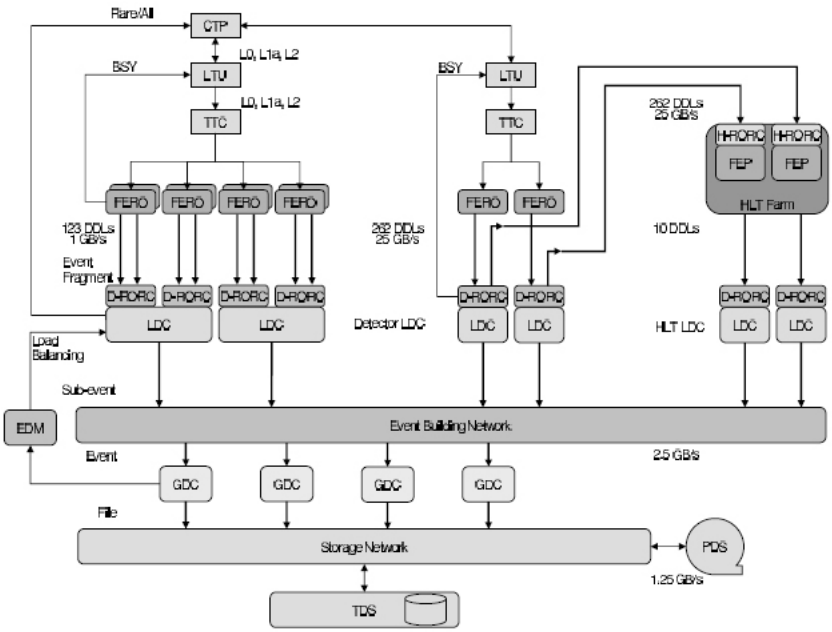

Figure 11: DAQ chain

is to ship the sub-events to a farm of machines (also commodity PCs) called Global Data Collectors (GDCs), where the whole events are built (from all the sub-events pertaining to the same trigger). Another major architectural feature of the ALICE DAQ is the event builder, which is based upon an event-building network. The sub-event distribution is driven by the LDCs, which decide the destination of each sub-event. This decision is taken by each

LDC independently from the others (no communication between the LDCs is necessary), but it is synchronized among them by a data-driven algorithm, designed to share fairly the load on the GDCs. The Event-Destination Manager (EDM) broadcasts information about the availability of the GDCs to all LDCs. The event-building network does not take part in the decision; it is a standard communication network (commodity equipment) supporting the well-established TCP/IP protocol. The role of the GDCs is to collect the subevents and assemble them into whole events. The GDCs also feed the recording system with the events that eventually end up in Permanent Data Storage (PDS). The HLT system receives a copy of all the raw data; generated data and decisions are transferred to dedicated LDCs.

3.5 Calibration

As was mentioned the TPC is very sensitive to outside effects like changing temperature or pressure. In order to run the TPC one has to have possibility to measure the drift velocity online and to calibrate the TPC. As was proved

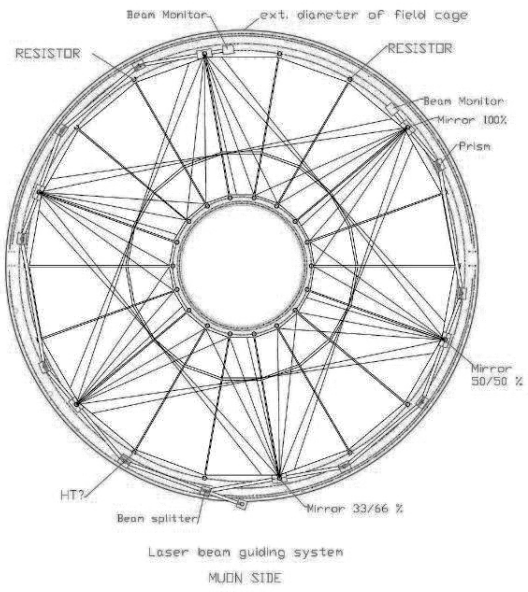

Figure 12: LASER used for calibration of the TPC [3]

in previous experiment a laser is very handy to online calibration. The main laser beam is led to the TPC where is divided using small mirrors to cover the whole TPC volume. The scheme of the laser beams inside the TPC is in Fig. 12. During normal run the laser will be fired and from the response of the TPC the drift velocity can be determined. This laser was also used during precommissioning to test response of chambers and electronics. One of first pictures of laser is in Fig. 13. In order to measure small fluctuations

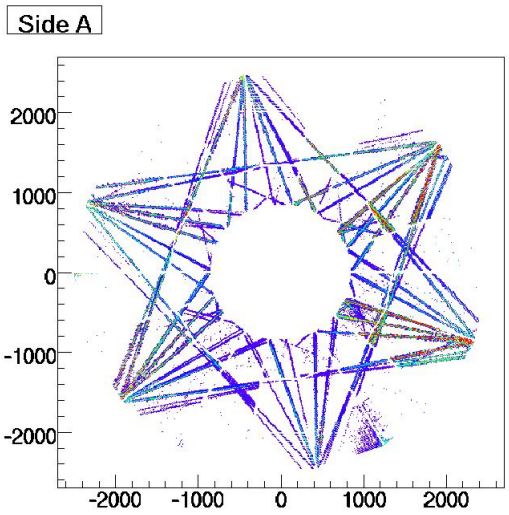

Figure 13: Real laser tracks measured in the TPC

in the gas composition small detector called a GOOFIE was built. The GOOFIE is measuring the drift velocity and also the gain. The drift velocity is obtained from the time difference between the drifting electrons produced by two emitting alpha sources, placed at known distances from a pickup detector. The field cage is operated at the unprecedented field of 400 V/cm, like in the TPC. The layout of the detector is in Fig. 14 [9]

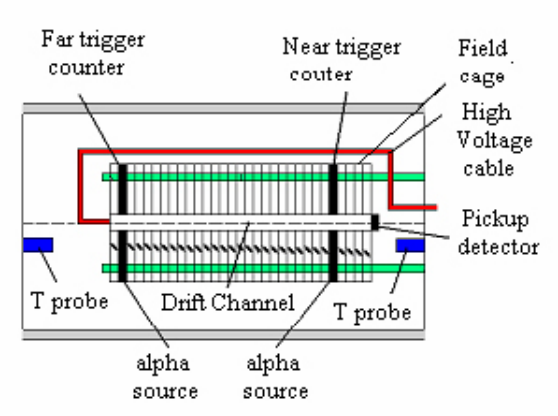

Figure 14: Scheme of GOOFIE [9]

4 PVSS

PVSS (Prozessvisualisierungs- und Steuerungs-System) is a SCADA (Supervisory Control And Data Acquisition) system used in CERN. It is used to connect to hardware (or software) devices, acquire the data they produce and use it for their supervision, i.e. to monitor their behavior and to initialize, configure and operate them. In order to do this PVSS provides the following main components and tools:

Archiving

A database is running. The data coming from the devices are stored, and can be accessed for processing, visualization, etc. purposes. Archiving Data in the run-time database. Connection to external (ORACLE) database is also possible.

Alarm Generation and Handling

Alarms can be generated be defining conditions applying to new data arriving in PVSS. The alarms are stored in an alarm database and can be selectively displayed by an Alarm display. Alarms can also be filtered summarized, etc.

A Graphical Editor (GEDI/NG)

Users can design and implement their own user interfaces (panels). **Scripts** Syntax used for scripts follows C syntax, with many implemented functions. This allows user to interact with the data stored in the database, either from

a user interface or from a 'background' process.

A Graphical Parameterization tool (PARA)

Is used to define the structure of the database and datapoints and to setup all kind of their options (archiving, alarms, etc.)

4.1 TPC Gating Grid PS

As was mentioned above, the ALICE TPC has a gating grid. To have possibility to open or close the gating grid one has to have three levels of voltage. For fast switching between open and close states, pulsers are used. As a voltage source ZENTRO LD2x150/1GF power supply was used. This power supply has two independent channels with output voltage 0-150 V. PS can be controlled remotely via RS232, using syntax from its firmware. As for all other devices in the ALICE experiment, the PVSS project has been made to control this PS. This project consists of three levels for three different types of users. A typical user doesn't need any knowledge of PVSS or PS. He uses final state machine (FSM) panel, from which he can control and set the PSs. Expert user can look inside the project and issue new commands for the PS. To facilitate this mode of operation a script in higher language was developed allowing the expert user to communicate with the PS by including simple line to script. The third and last level is for real experts and allows change the syntax itself. The scripts from this PVSS project are attached to this work. In order to communicate with PS one has to open communication channel, set COM port number, bandwitch etc. After communication it is preferable to close channel. This is protection against some hang up problems. In the case that the PS replies for sent command, reading of channel is repeated till CR+LF appears. After this channel is closed. All this is done automatically in included syntax. If reply is awaited script waits for some time and in case of successful reading value is stored in appropriate datapoint. When no reply appears, NO CONTROL flag is raised (waiting for reply is only way how one can check that connection exists). The FSM digram of this project is in Fig. 15. Basic state is OFF. One can go there from NO_CONTROL state or from STBY_CONF state. In case of problems with communication, script

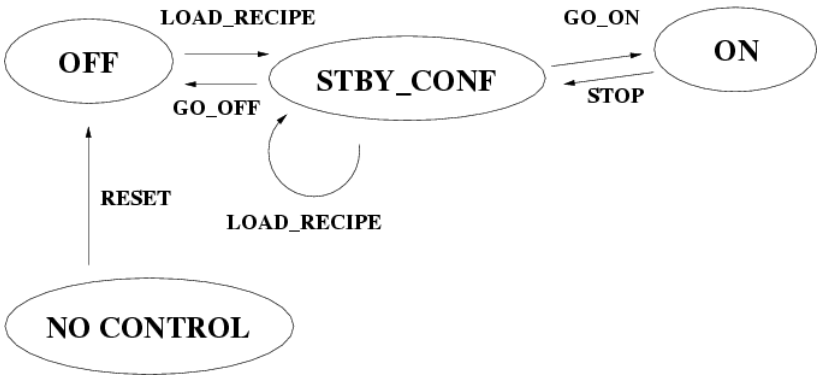

Figure 15: FSM states diagram of gating project

automatically tries once in given period communication again. If communications is established state switches change to OFF. NO_CONTROL state has been included and is raised in case of communication problem between PS and PVSS. When PVSS detects too many same errors, whole project can be blocked and restart of project is needed. In state OFF all settings are set to 0. The PS is set via action LOAD_RECIPE. In future all settings will be stored in ORACLE database. Nowadays the local database is used instead. In database many settings can be stored (in case of gating project probably only one will be needed). User can load different recipe using key word (name of setting). Communication with database was set and is functional. One can change settings in STBY_CONF state without going to OFF. In this state there is no output voltage on PS. After GO_ON action output voltage is ON and state switches to ON state.

Scripts for reading and setting real values are included in project. Values are read every 5 s. Higher frequency of reading can lead to problem with too busy communication line and some commands can be lost or executed with delay. With frequency 0.2 Hz the project was tested for month without any problem.

For case that some script dies during operation the watchdog function is included to control all scripts. With this safety is improvement, user can see immediately problem and script can be restarted.

4.2 GOOFIE

In order to know exact gas composition the small model of the TPC has been made and drift velocity is measured. This model is called GOOFIE. It was decided control GOOFIE as all other parts via the PVSS. PVSS PC DIM (Data Interface Management) was used for communication between PC responsible for computing drift velocity from measured values and control . It is also foreseen to control the HV PS of GOOFIE via PVSS. In the end this PS will have hardware interlock, fast software interlock on GOOFIE PC, and PVSS interlock with little longer response time. Code used in Gating project can be modified and reused again in GOOFIE project.
DIM server has been successfully set on GOOFIE PC and communication with PVSS client has been established. So one can use connection to PVSS database and save data there.
As was mentioned above, all parts of the ALICE experiment will be controlled by PVSS projects, which will be integrated in one big ECS (Experiment Control System) tree. Human operator will have full control of every part of project in very easy and intuitive way.

5 TPC Commissioning

In the autumn 2006 the TPC was set up and precommissioning was started. Huge effort was done by inputing all electronics and services needed to run them. The TPC was in clean room on the surface in the ALICE point in CERN. A cooling for the electronics was installed and gas system was running. So there were all necessary services to run the TPC. Services for electronics were only temporary, hence there was no way to run more then two sectors at time. Above and under the TPC the scintillators were installed, providing trigger for cosmic. Test which followed were focused mainly to chambers and their behavior and stability. During commissioning one chamber with broken anode wire was replaced. The problem with attachment of the chamber to the TPC was discovered during this procedure. It was necessary to uninstall not only the broken chamber, but also two neighboring chambers. Hence new attachment system was evolved and now can be chamber exchanged easier. One have to understand that exchanging of chamber is still very delicate operation, very time consuming. One has to open the TPC hence change gas to nitrogen and after procedure change it to working mixture again.

During tests the trip behavior of the chambers was observed, but in the end all chambers worked on their nominal voltage. The tripping characteristic of chamber was studied deeper and characteristic of HV PS which is used is mentioned in Sec. 7.

Two day program of testing included ramping up to nominal voltage, stability test, laser test and cosmic test. To watch data the Online Monitor from Stephan Kniege was used. On Online Monitor (OM) the noise in top corners of the OROCs appeared (Fig. 16). The fourier decomposition to the frequency domain showed that the main source of the noise has frequency 2.5 MHz. This corresponds to the frequency of emptying a buffer on ALTRO. The sampling frequency is 10 MHz, from four 10 bit words new 40 bit is created and then send to DAQ. The current consumption during emptying the buffer causes change in a ground potential which is common for both digital and analog part of the FEC. Hence we can see the result as a noise. In

order to avoid this one can use so called desynchronization, which means not to start all ALTRO chips on FEC simultaneously. ALTROs are divided to four groups which are started with 100 ns delay respectively. After applying desynchronization the noise level dropped down rapidly. Together with new better grounding scheme the noise in RMS was under 1 ADC as required (10 bits for 2V $\rightarrow$ 1 ADC $\sim$ 1000 e $\sim$ 1.95 mV).
As was mentioned above all the chambers were tested in the clean room for two days and they are tested intensively during winter 2007/2008.
In January 2007 the TPC was lowered to cavern. After this big effort to operate all the services was made. Preparation of configuration scripts for electronics and PVSS project for DCS boards were also in progress. In June 2007 series of tests on C side of the TPC (one close to muon detectors) were in progress. There were 8 sectors tested at once. During these tests the new LV PSs Wiener PL512 were used. Opposite ones used in clean room (PL 500) these are water cooled. Some data were saved for future analyze using very low trigger frequency - typically 0.5 Hz. For the first time elec-

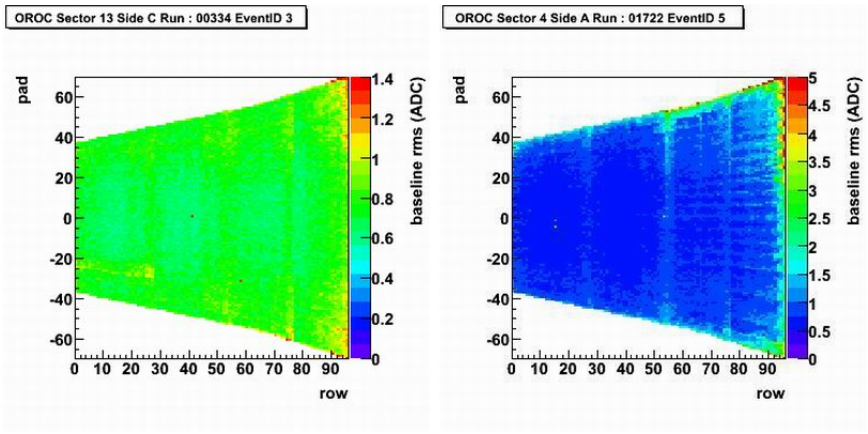

(a) Old power supply PL500 (b) New power supply PL512

Figure 16: Noise in OROC corner after desynchronization (notice different scale)

tronic configuration was done automatically via DDL and many tests with DCS were done. Data analyzing showed that the noise problem reappeared.

High level of noise in corners of OROC chambers appeared again. This time however, the main frequency wasn't 2.5 MHz. Hence the desynchronization didn't solve the problem completely. A question from where the noise come was discussed intesively during the summer 2007. The new PS was suspected as the most obvious source. In order to prove that two sectors with old PSs were run on A side in August. It showed that in this case the noise is the same as it was in the clean room and desynchronization solves the problem. Comparison of data with old and new PSs are in Fig. 16. One should mention different scale in these two figs. With new PS even with maximum of 5 ADC counts there is still saturation in corners, however for old the maximum is set to 1.4 ADC. In Fig. 17 one can see histogram - noise distribution in ADC in RMS. Fig. 18 shows fourier decomposition of signal in pad with highest noise. It is clearly visible that with new PS noise is higher and there are new frequencies which cause it.
Other possibilities like some disruption from cables were also explored, but was found as wrong. There is no correlation between position of cables and noise pattern.
In order to make analysis easier the minor changes in OM (Online Monitor) were made. Script looks for pad with highest noise level and make fourier decomposition there.

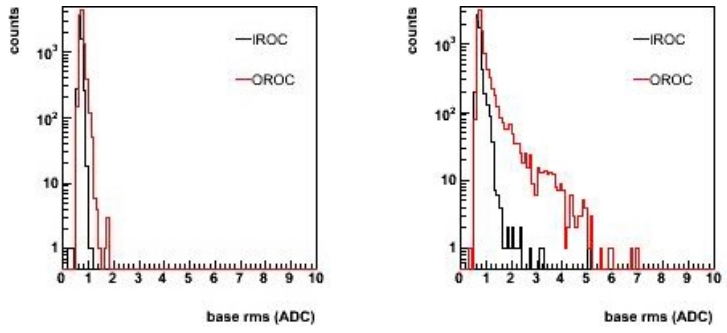

(a) Old power supply PL500 (b) New power supply PL512

Figure 17: Noise in OROC corner after desynchronization - RMS

After acquiring such results the measurement on the new PS output were

made. The results are in section 5.1
In August there was testing of a A side of the TPC. Nine sectors were tested in one time. This time the DCS for reading values of electronics was used. The FECs send their voltage, temperature and FSM state. Unfortunately high number of channels which have to be read caused some problems and crashes of the PVSS project. So that the data received via DCS weren't very reliable. Although these problems occurred, there was noticed that voltage on electronics is lower then should be and it is far from stable. The jumps of 0.7 V were observed. In the end the source of all these problems was found. And it is noticed in section 5.2.

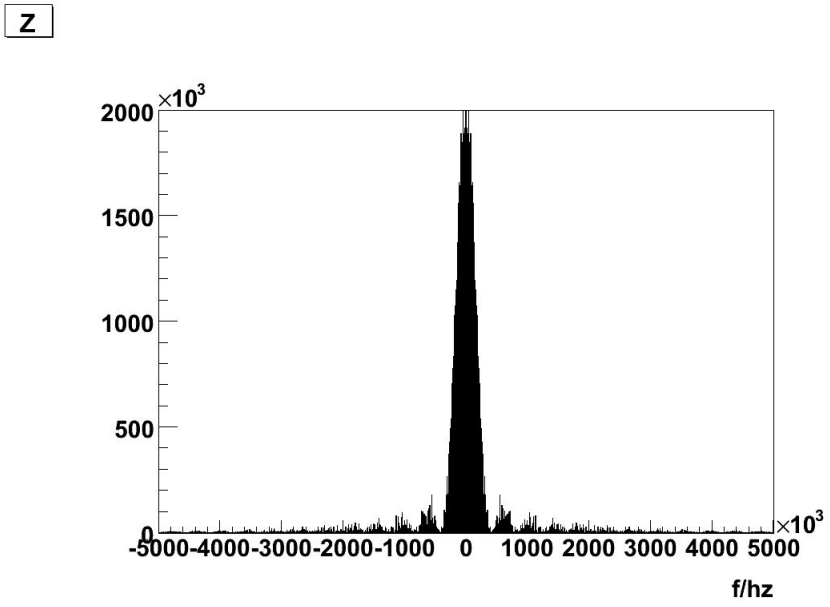

(a) Old power supply PL500

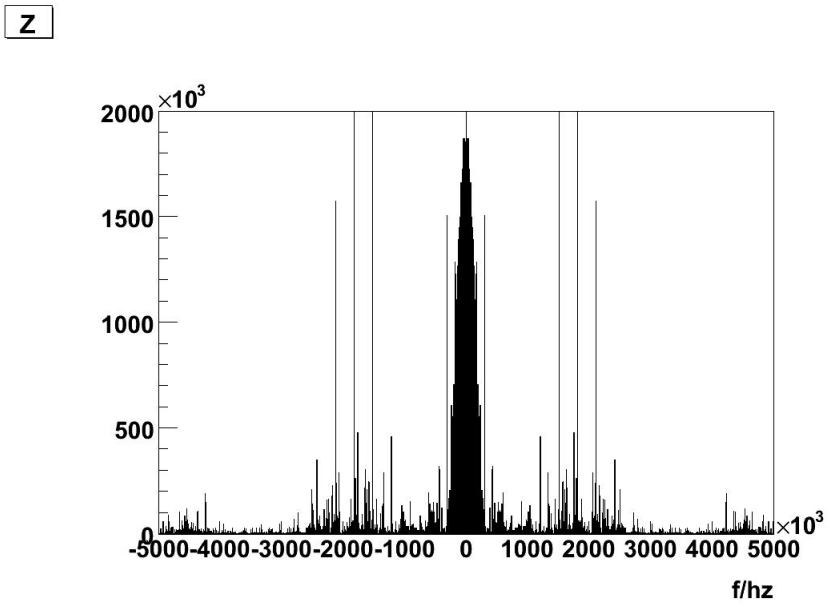

(b) New power supply PL512

Figure 18: Noise in OROC corner after desynchronization - Fourier power spectrum

5.1 New PS output

The new PS PL512 was tested in compare to old one. Series of test were done during September. The results are shown in and Fig. 19.

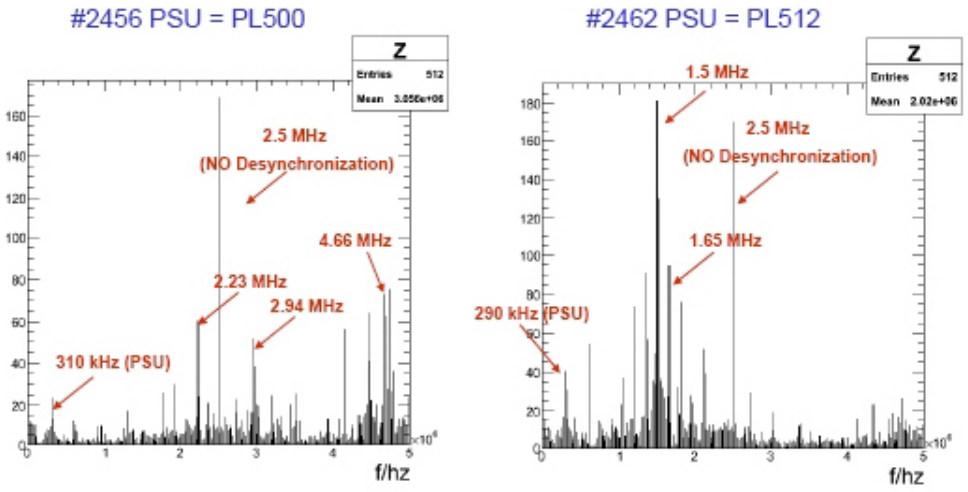

(a) Old power supply PL500 (b) New power supply PL512

Figure 19: Noise in frequency domain

5.2 BUSBAR problem

FEE is powered by LV PS. From this PS thick high current cables lead to sectors, where are connected to busbars, which are bars of copper on the side of each sector. (Fig. 20) On the busbar there are connectors which distribute power to all the electronics. The problems with too high voltage drop measured on the electronics led to checking this connectors. It showed that even after cleaning these connectors the voltage drop is still too high. (Tab. 3) One of connector was dismounted and the problem was found. The soldering on these connectors was made on wrong place, so that the contact was disrupted. The problem is shown in Fig. 21. As a consequence of this discovery, all busbars were removed and repaired. This procedure was very time consuming and 8 people were needed. Even though only one sector per

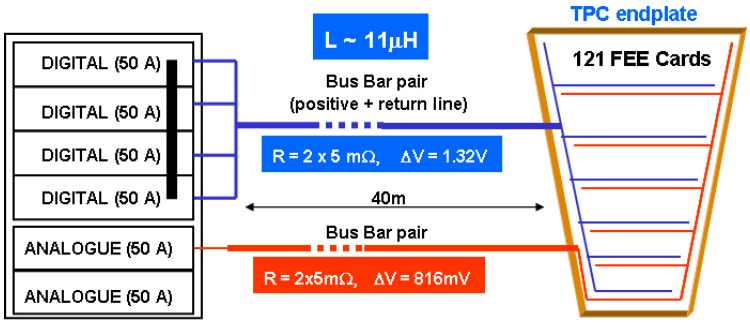

Figure 20: Power scheme for the TPC sector

Sector	U-busbar – Usense (mV)		Umax-Umin (mV)	
	Digital	Analogue	Digital	**Analogue**
A00	180	140	130	150
A01	145	103	100	60
A02	160	117	100	40
A03	180	110	90	90
A04	200	140	280(*)	60

(*) After 2nd cleaning

Table 3: Voltage drop after connectors cleaning

day was repaired. The connecting scheme was also changed in order to reach better stability. (Fig. 22)

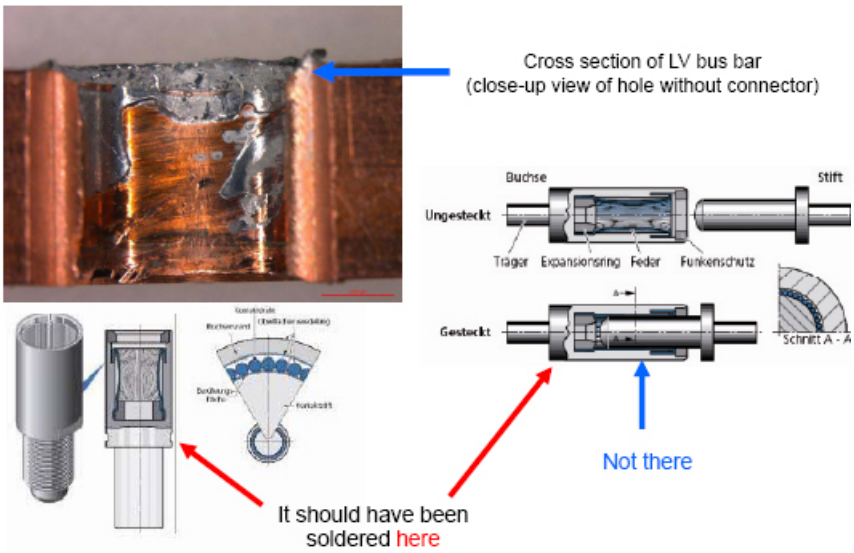

Figure 21: Faulty soldered connector on busbar

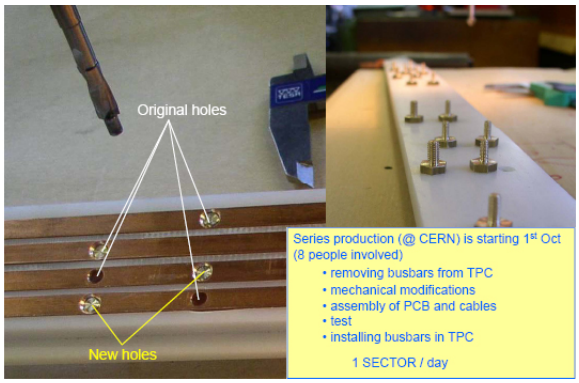

Figure 22: New connection scheme on busbar

6 Cooling

As was mentioned above the ALICE TPC is very sensitive to temperature. In order to have stable drift velocity, it is necessary to keep the temperature changes under 0.1 K. This task is really big challenge. On the both endcaps of the TPC there are FEE with output about 30 kW. The TPC will be also surrounded by other detectors, namely by ITS and TRD, which will also dissipate the huge amount of heat. To protect the TPC against these effects the sophisticated cooling was developed. As a coolant normal water was chosen as the best one. The problem with the water is clear, if some leak occurs in the cooling circuit it could destroy whole electronics. Hence to avoid this, the underpressure system was developed. The system works as the name tells in pressure lower then atmospheric one. Thus in case of leak the water should not go away from circuit but rather back to the tank. During testing in summer 2007 the problem in this solution was found. When the artificial leak was created the system remained under pressure for only 10 s, after this big leak occurred. It showed up that the sensor in tank has no chance to detect any leak and stop pump to prevent splitting water everywhere. In order to guarantee the leak detection a pair of sensor had to be mounted to each TPC sector. When these sensors detect change in pressure the PLC sends signal to cooling plant and stop the pump. This system is fast enough to prevent splitting water and because of PLC is very reliable.
In order to keep thermal changes as low as possible every FEC has its own cooling. On top of it every chamber is cooled as well. The cooling envelope of the FEC is in Fig. 23. One can see that only one side of the cooling envelope is actively cooled. It was tested that when there is good thermal bridge between these two sides, this cooling is sufficient. To shield the heat from other detectors. The cooling planes are around inner and outer cylinder of the TPC.[12] Is worth of mention that cooling water is provided for each sector separately, so the cooling temperature can be set differently on different sectors, but not for chambers, so the temperature for IROC and OROC has to be same.
in Fig. 24 one can see the time evolution of temperature during the test. The

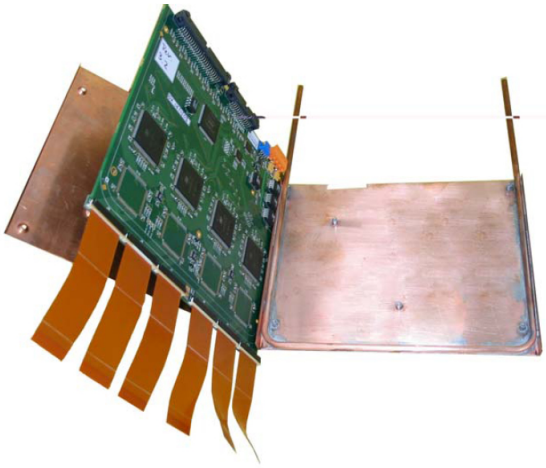

Figure 23: FEC in cooling envelope

switching electronics off and on is clearly visible. More detailed results of test are for example in [12]. The problematic of cooling is rather complicated, here was only briefly described few aspects.

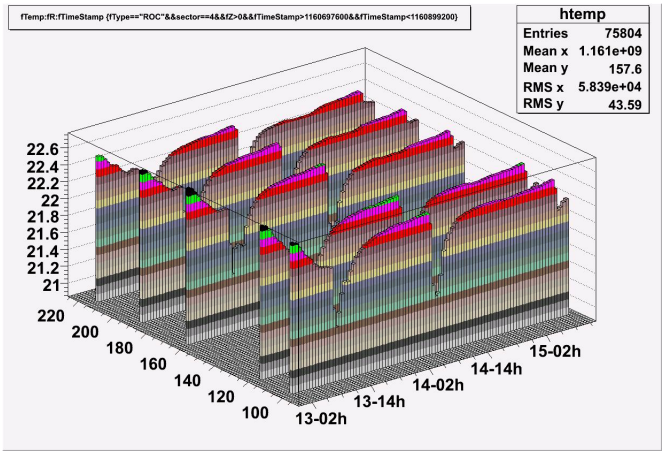

Figure 24: Temperature in time on one sector

7 ISEG Power Supply

Multiwire chambers from the ALICE TPC are powered via HV PS ISEG EHQ 20 025p204 H. High voltage around 1400 V is sent on anodes. During lab tests of chambers spark discharges (Fig. 25) were observed. The reason for this sparks is yet unknown, but one has to be ready to handle them. ISEG power supply (PS) provides tripping, which we tested. The output

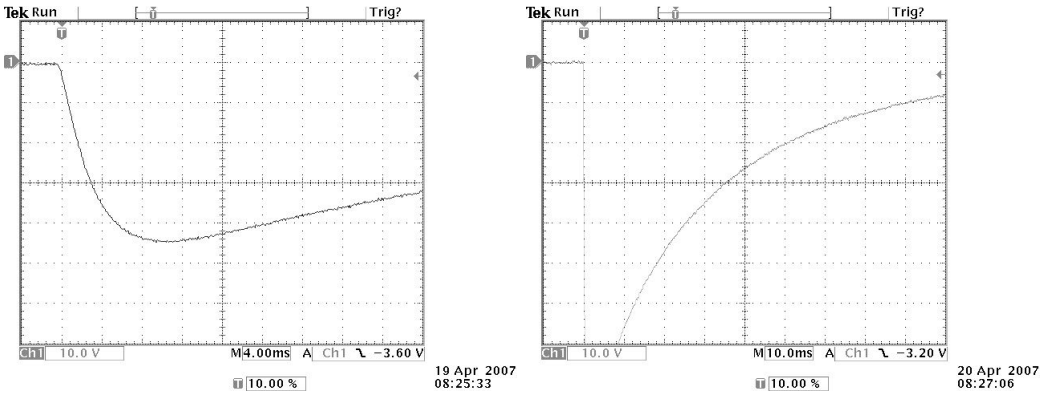

(a) Discharge with osciloscope set to 10 V and 4 ms

(b) Discharge with osciloscope set to 10 V and 10 ms

Figure 25: Example of discharges during IROC tests

current is internally measured via comparator with threshold level which one can manually set on the power supply. Our requirement is protection of chambers, but not tripping during normal run, even with high multiplicity events. During the test we used a circuit based on a switching relay, which is shown in Fig. 26. The relay is opened with a 3 V fast pulse and can withstand currents of 1 mA without any problems or leakage currents. The minimal length of pulses needed to open the relay is 830 μs.

We have been changing the R1, R2 of the circuit in order to change amplitude of the discharges. Resistors R1 and R2 can be varied to tune the amplitude of the discharge pulse, and R2 is tuned to fit the scope signal into its dynamic range. The output voltage of PS was 300 V.

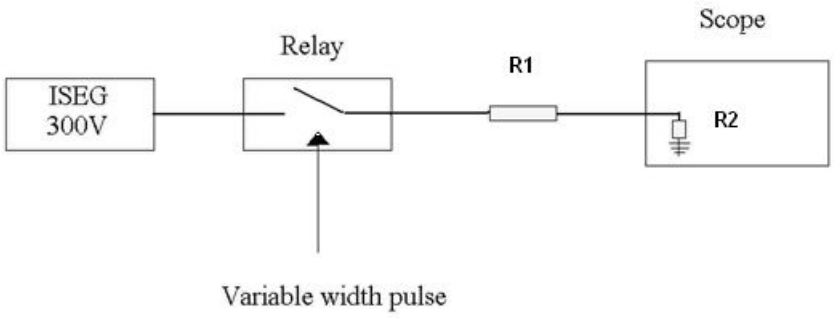

Figure 26: Schematic diagram of the circuit used

7.1 Minimum duration of pulse to trip

We tested what is the minimum length of discharge for a given amplitude on which PS reacts with different thresholds. The results are shown in Fig. 27. The relative threshold is the trip limit setting on PS divided by amplitude of discharge. We made measurements for two different amplitudes: 60 μA and 120 μA. A discharge two-times bigger than the trip limit won't trip the PS if it is shorter than 3.3 ms.

7.2 Response time of PS

The relay was opened for infinite time and we measured the time to trip as a function of relative threshold. The results are shown in Fig. 28. You can see that PS behaves nearly same for large variety of amplitudes of discharge. This plot looks the same. It actually shows the same as Fig. 27, but measured in a different way.

7.3 Stability under real load

In real experiment the PS has to withstand events with frequency 200Hz which produce each about 100 μA current for 100 μs. The minimum time which is needed for opening the relay is 830 μs. That's why we decide to put pulses 1 ms, which is 10 times longer than the real ones. We also simulated

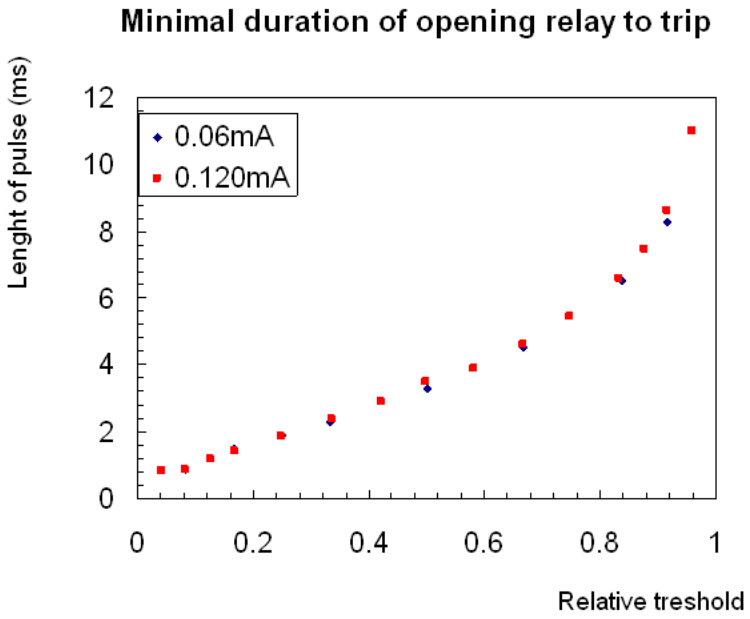

Figure 27: Minimum duration of discharge to trip PS, i.e. the shortest open relay time which leads to trip

randomness of events, so that the frequency of pulses wasn't constant, but keeping it at 200 Hz on average. We used setting with 0.150 mA / 200 Hz / 1 ms. With this parameters there was no trip for day with trip limit on 70 μA. During test one can see permanent current around 13 μA drawn from PS. The settings with 1 mA / 20 Hz / 1 ms and 1 mA / 200 Hz / 1 ms were also tested. Even with very drastic settings with 1 mA peak consumption was set up stable for some hours. In this case one can see permanent current up to 80 μA. The output voltage is not stable anymore on 300 V, but its value jumps between 280 - 340 V. One should remember that PS will work with voltage around 1400 V. Testing with 300 V is rather low and characteristic can be changed, but better relay is not available. In summary one can say that PS is capable of handling conditions, which will be during real experiment.

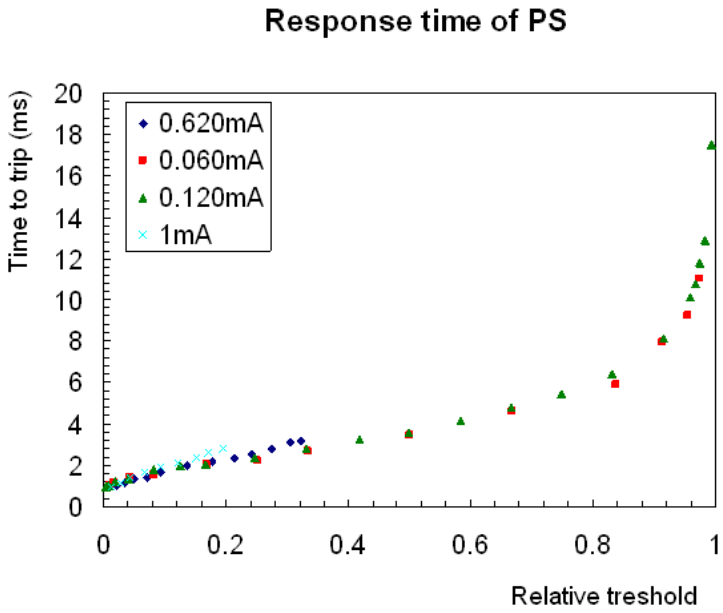

Figure 28: Time to trip, i.e. time of reaction of PS with relay opened for infinitely long time

7.4 Minimum threshold for real experiment

Safety of chambers has highest priority, hence it is reasonable to have the trip limit set as low as possible. In this measurement the lowest threshold was seek. Discharges with amplitude 0.1 mA (like real events) and 1 ms long (ten times longer than real events) at 200 Hz frequency (real frequency) were set up. For trip limit 29 μA there was no trip during night. That means one can set very low level of trip limit, which will protect chambers, but will not trip even with high multiplicity event.

ISEG EHQ 20 025p204 H PS's tripping behavior is satisfying. It protects chambers well and does not trip without reason.

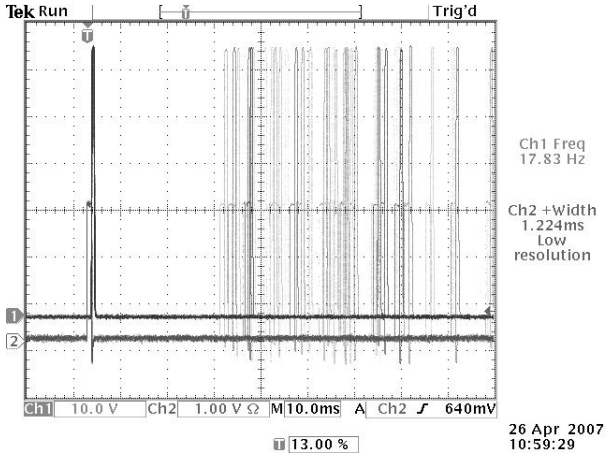

(a) Frequency 20 Hz

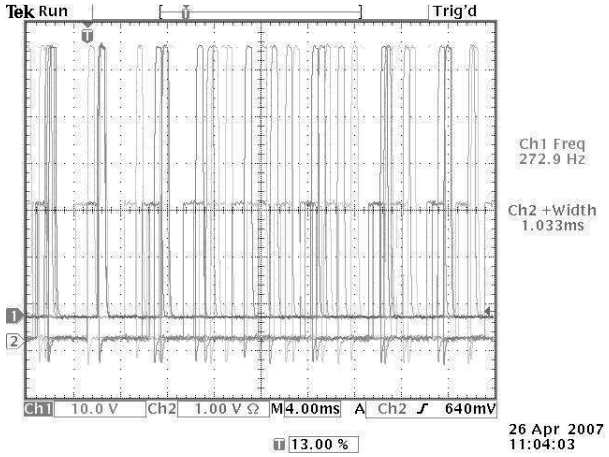

(b) Frequency 200 Hz

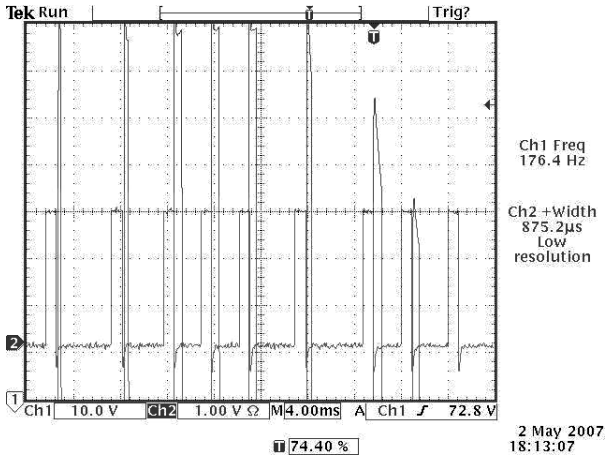

(c) Trip in 200 Hz

Figure 29: Real load testing - discharge 1 mA

8 Summary

During the last year, the huge amount of effort was made to test and run the ALICE TPC. Some very interesting problems were discovered and most of them were solved. As a member of the ALICE TPC group at GSI I was responsible for topics mentioned in Sec. 4 - 7. In addition, I participated on many installation works during the TPC precommissioning and commissioning. We have installed all electronics and services necessary to run the TPC. Moreover, I assisted at shifts during which were collected e.g. first cosmic data of the TPC or was discovered a voltage drop on the electronics.
I was responsible for development of PVSS project for the Gating Grid PS and for the the GOOFIE drift velocity monitor. The former was finished, installed, and tested. The later was finished and the communication between PVSS PC and GOOFIE PC was established. Tests will be performed as soon as the GOOFIE software is finished.
The tests of HV PS ISEG, which I carried out, proved that this PS is well chosen and is capable of handling all the possible situations which can occur during the experiment.
The observed noise problem, described in Sec. 5, results in lost of resolution in particular parts of the TPC. In order to discover the source of that noise, I have analyzed the noise data. The results were presented on the TPC meetings. During the data analysis I have modified the Online Monitor software to make the future analysis easier. Up to now the noise problem wasn't solved; however, it is highly probable that some upgrade of PSs will fix it in next few months.
In the middle of the year 2008 the LHC should start first beam. The TPC will be ready in that time. During the first half of the year 2008, various tests will be performed. The read-out chambers under high voltage together with the very high voltage of the field cage will be tested first. Afterwards, the krypton calibration of the TPC will take place. Finally, the DAQ will collect data considering different settings of electronics.
Results of this thesis will be used during all of the mentioned phases.

References

[1] N. Cabbibo, G. Parisi, Phys. Lett. B59 (1975) 1353.

[2] F. Karsch, Lect. Notes Phys. 583 (2002) 209 [hep-lat/0106019]; F. Karsch, E. Laermann, hep-lat/0305025; E. Laermann, O. Philipsen, hep-ph/0303042.

[3] Technical Proposal for A Large Ion Collider Experiment at the CERN LHC, CERN/LHCC/95-71, LHCC/P3, 1995.

[4] Technical Design Report of the Time Projection Chamber, CERN/LHCC 2000-001, ALICE TDR 7, 2000.

[5] C. Garabatos, The ALICE TPC, Nuclear Instruments and Methods in Physics Research A 535 (2004) 197Ű200.

[6] J. Wiechula et. al, High-precision measurement of the electron drift velocity in NeŰCO2, Nuclear Instruments and Methods in Physics Research A 548 (2005) 582Ű589

[7] ALICE Collaboration, ALICE: Physics Performance Report, Volume I, J. Phys. G: Nucl. Part. Phys. 30 (2004) 1517Ű1763.

[8] L. Musa et. al, The ALICE TPC Front End Electronics, http://ep-ed-alice-tpc.web.cern.ch/ep-ed-alice-tpc/doc/papers/NSS2003.pdf

[9] J. Castillo et. al., Experience with the Goofie during the TPC commissioning, http://www.gsi.de/ informationen/wti/library/ scientificreport2006/ PAPERS/INSTRUMENTS-METHODS-33.pdf

[10] C. González Gutiérrez et. al., The ALICE TPC Readout Control Unit

[11] R. Esteve Bosch et. al., Readout Control Unit of the Front End Electronics for the ALICE Time Projection Chamber

[12] S. Popescu et. al, Experimental Evaluation of the ALICE TPC Front-End Electronics Cooling Strategy, ALICE-INT-2005-001, 2004